IEEE Copyright C. Martín-Rubio et al., "Magnetic Characterization of Permalloy Nanodome Surfaces on Flexible PEEK/TiO2 Vertical Nanotubes Composites," in IEEE Transactions on Magnetics, vol. 59, no. 2, pp. 1-6, Feb. 2023, Art no. 6500106, https://doi.org/10.1109/TMAG.2022.3212831

Magnetic characterization of Permalloy nanodome surfaces on flexible PEEK/TiO_2 vertical nanotubes composites

C. Martín-Rubio[1], A. Rivelles[2], M. Schneider[3], J. C. del Hoyo[4], V. Privitera[5], M. Worgull[3], M. Maicas[2], R. Sanz[1]

[1]Payloads and Space Science Department, National Institute for Aerospace Technology, Torrejón de Ardoz, Spain
[2]Institute for Optoelectronics and Microtechnologies, Polythecnic University of Madrid, Madrid, Spain.
[3]Karlsruhe Institute of Technology, Institute of Microstructure Technology, Germany.
[4]Materials and Structures Department, National Institute for Aerospace Technology, Torrejón de Ardoz, Spain.
[5]Institute for Microelectronics and Microsystems, CNR, Catania, Italy.

Poly-ether-ether-ketone (PEEK) composites present outstanding physical and chemical properties, including radiation tolerance and compatibility with vacuum and additive manufacturing processing. Applications of PEEK range from biomedical to aerospace. Controlled 3 dimensional nanostructuring arises as a powerful approach to generate new phenomena suitable for technological applications. In this sense, we target to synthesize robust and shapeable magnetic nanocomposites, for sensing and electromagnetic shielding applications. For this aim, we synthesized and characterized Permalloy (Py, $Ni_{80}Fe_{20}$) nanostructured surfaces on PEEK/TiO_2. These nanocomposites were synthesized by scalable and high throughput compatible fabrication approaches: Anodization (TiO_2 nanotubes) and hot embossing (thermal nanoimprint). The resulting nanocomposites are shapeable, stable below 300 ºC and vacuum compatible. Their surfaces compose TiO_2 nanodomes filled by PEEK. Py layers (15 nm) were sputtered on NC and flat PEEK films. The characterization included SEM, AFM, ISO-2409 Adhesion Tests, hysteresis loops and First Order Reversal Curves. The results revealed that both type of films keep stable characteristics after bending cycles, and noticeable modifications of the magnetic global response and local interactions generated due to the 3-dimensional nanostructure.

***Index Terms*— Magnetic Characterization, Nanostructures, PEEK, Permalloy, TiO_2.**

I. Introduction

3 Dimensional (3D) nanostructuring, revealed as a powerful and versatile tool for the study of curvature and topological effects of magnetic materials [1]-[4]. Moreover, future applications of these 3D nanostructures e.g. magnetoelectronics, for electromagnetic shields/absorbers, GHz filters or even non-Boolean computing, demand new synthesis approaches for extended capacities. These new capacities include bendability [5], e.g. for shapeable electronics/sensing; resistance to rough environments of temperature and vacuum e.g. aerospace[6]; and the capacity to synthesize 3D nanostructures at a relative large scale (cm^2). Bendability and robustness can be ideally achieved using technical polymer substrates as matrices. Polyimide (e.g. Kapton©), Cyclo Oleofins and Poly-Ether-Ether-Ketone (PEEK) [7] are good examples of robust and bendable substrates. Although Polyimides [8]-[10] and Cyclo Oleofin [11]-[12] films have been employed as substrates for magnetic applications, PEEK, and its composites, are preferred for applications involving mechanical loads and/or chemical stability, due to its outstanding physical and chemical properties. PEEK is biocompatible, radiation tolerant, compatible for cryogenic and ultra-high-vacuum environments (low degasification and low thermal conductivity), and adequate thermoplastic for Fused Deposition Modelling. Nowadays, the applications of PEEK ranges from medical implants [13] to space fields [14], [15]. At nanoscale, the infiltration of melted thermoplastic polymers in nanostructured templates is a widely employed approach to generate nanostructured polymer materials [16]. This allows the study of nanoconfinements effects on their functional properties, for instance optical or bioactive, and also their use as substrates for magnetic nanostructures [17]. However, this approach may consume days, including the template synthesis and infiltration step, and often the sacrifice of the template. Hot embossing[18] is an efficient high throughput technique for micro- and nanopatterning thermoplastic materials, when the appropriate template or master is availed. Nevertheless, the necessary resources for the master fabrication, the aspect ratio of the templates/masters and the adhesion of the polymer are limiting factors for up scaling and decrease the processing time and costs. Therefore, the use of self-ordered systems as templates provides advantages under time and costs criteria. Some anodic oxide layers, as porous anodic alumina, have demonstrated for decades their versatility as templates for hexagonal ordered magnetic nanosystems [19], such as nanowire arrays [20], nanodome surfaces [21]-[23] and more recently for 3D magnetic nanonetworks [24]-[25]. Nevertheless, their use as templates implies time-consuming fabrication steps, highly toxic chemical reagents and hazardous waste. In the majority of cases the synthesis of ordered porous alumina demands costly high purity Al (>99.999%). Its chemical synthesis comprises an initial electropolishing and a double anodization process, resorting to harmful chemical reagents. In addition, the complete process extends for long periods (days) under tight conditions of temperature and stirring. Moreover, the separation of the porous alumina from the Al foil implies the loss of the foil and additional use of toxic reagents. The resulting porous alumina layers are rigid and brittle making them difficult to handling for further uses. Alternative nanostructures can mitigate some of these inefficiencies and drawbacks. In this sense, anodic TiO_2 nanotube layers represent a valid choice for applications where long range ordered nanostructures are not a premise. Anodic TiO_2 nanotubes layers have been extensively studied due to their suitable properties in fields ranging from biomaterials to energy and environmental remediation [26].

IEEE Copyright C. Martín-Rubio et al., "Magnetic Characterization of Permalloy Nanodome Surfaces on Flexible PEEK/TiO2 Vertical Nanotubes Composites," in IEEE Transactions on Magnetics, vol. 59, no. 2, pp. 1-6, Feb. 2023, Art no. 6500106, https://doi.org/10.1109/TMAG.2022.3212831

Their synthesis process can be applied on low purity Ti (<99.9%) without previous electropolishing. In addition, the anodization of Ti is performed at room temperature, and resorts to safer reagents compared to those for porous alumina. Moreover, TiO_2 nanotubes reaches growing rates >10 µm/hour. Therefore, the use of TiO_2 nanotubes layers reduces the environmental impact, reduces the time and economic costs at laboratory scale, paving the way for further up scaling.

The aim of this work is to present the first results on a new approach that optimizes the fabrication process of robust and bendable 3D magnetic nanostructures, Permalloy (Py, $Ni_{80}Fe_{20}$) nanodomes and its comparison to those obtained on flat surfaces.

II. MATERIALS AND METHODS

A. Materials and synthesis methods

The synthesis process is summarized in Figure 1. The synthesis of TiO_2 nanotubes consisted in the anodization of Ti sheets (99.6% Goodfellow), with exposed areas of 7 cm^2 at 50 V (DC) using an electrolyte composed by Ethylene Glycol, NH_4F (0.5 wt%, anhydrous 99.8%, Sigma Aldrich) and Deionized water (8.0 wt%). The anodization was performed at room temperature with no stirring. Then the obtained TiO_2 nanotubes on Ti foil were submitted to thermal annealing under N_2 atmosphere for 1 hour at 400 ºC.

PEEK foils (0.1 mm thick Sigma Aldrich) were cleaned (degreased in ultrasound bath) and used without additional treatments, both for hot-embossing and in sputtering processes.

FIG. 1 HERE

The synthesis steps are depicted in Fig.1. Briefly, they were carried out by placing the PEEK foils on the anodized Ti surfaces containing the TiO_2 nanotubes. Then, 25 kN at 365 ºC (note that the melting temperature of PEEK is 360 ºC), were applied for 1 minute. These conditions force the melted PEEK to flow inside the TiO_2 nanotubes. After the cool down to room temperature (approximately 5 minutes) the PEEK foils were stripped off from the anodized Ti sheets. After this step, the Ti sheet is availed to be reused again in another anodization process [26]-[27]. Since this is a mechanical process the use of chemical etchants is not necessary and thus, further economic and environmental costs are reduced. Then, the TiO_2 nanotubes /PEEK nanocomposites (NC), were submitted to a manual soft polishing/cleaning process of the surfaces, using a cloth impregnated with SiO_2 suspension (0.05 µm), and subsequent cleaning in deionized water in an ultrasound bath. 1x2 cm^2 pieces of NC and PEEK foils were cut with scissors to be used as substrates for Permalloy (Py) sputtering

Py target from (Kurt Lesker) was used for DC magnetron sputtering on NC and PEEK foil. The conditions were chosen in order to minimize the stress induced during the growing process. Ar pressure of 1.5×10^{-3} mbar and a deposition power of 100 W. The base pressure was lower than 10^{-6} mbar, and the distance from target to substrate was about 15 cm. The Py growing rate was previously characterized resulting in 0.14 nm/s.

B. Characterization Techniques

SEM imaging was performed by a field emission Zeiss Supra 25 microscope.

Surface nanotopography characterization was performed by an AFM (Nanoscope) in tapping mode.

The hysteresis loops and First Order Reversal Curves (FORC) were performed by a vibrating sample magnetometer (VSM, model Microsense EZ-7). Hysteresis loops were performed at several angles from, in-plane (0°) to out-of-plane (90°), while FORC were measured in in-plane orientation (0°). After a first round of magnetic measurements the samples were mechanical bended in a rod (1 cm radius, keeping the Py layer outbound). After 10 bending cycles, the hysteresis loops were measured again (in plane and out of plane). Final Adhesion tests of sputtered Py on the surface of PEEK and NC were performed following the indications of ISO-2409 standard [28] adapted to the limited size of the samples.

III. RESULTS AND DISCUSSION

Fig. 2 a) shows a macroscopic image of the NC after the stripping off (Fig.1 c). The dark area correspond to the TiO_2 nanotubes. The as obtained TiO_2 nanotubes layers from anodization exhibit a whitish color. Nevertheless, due to the thermal annealing they turned dark following crystallization from amorphous to Anatase phase [26]. In addition, thermal annealing generates thermal oxide within the interface between the bottom of the TiO_2 nanotubes and the Ti surface (Fig 1 a). Remnants of this thermal oxide adheres to the nanotubes bottom [27]. The surface and cross section (mechanical cut) of the NC were characterized by SEM after the soft polishing step. The soft polishing process succeeded to expose the nanodome surface of the bottom of the TiO_2 nanotubes, now on the surface of the NC (See Fig 1. c and Fig. 2 b). The average diameter of the nanodomes was 120±30 nm. The SEM cross section images (Fig. 2 c) show a total length of TiO_2 nanotubes of 11±1 µm. Fig. 2 c) shows also bundles of PEEK nanowires and sections of broken TiO_2 nanotubes generated by the mechanical cut.

FIG. 2 HERE

Subsequently to the sputtering of Py on bare PEEK (Py/PEEK) and on NC (Py/NC), the surfaces of the samples were analyzed by AFM. The AFM images of Py/PEEK sample revealed the existence of surface crinkles, with <1 µm height but mm length, coming from the original polymer surface (see Fig.3 a). Nevertheless, the resulting RMS roughness of the Py in this sample was 2.5 nm (Fig. 3 b) [29]-[34]. The AFM images of the surface of Py/NC confirmed that the deposited 15 nm thick layer of Py on the NC surface reproduced the conformal nanodome topography (Fig. 3 c and d). The image analysis of Fig.3 c) resulted in diameter distribution of the Py (Fig. 3 e) of 100±10 nm. This value is compatible but slightly lower than

that obtained from SEM images of bare nanodomes. This deviation can be ascribed to the different imaging techniques and statistical fluctuations.

FIG. 3 HERE

The results of the magnetic hysteresis loops are presented in Figure 4. The hysteresis loops performed in-plane (0º), Fig. 4 a) and out-of-plane (90º, Fig. b) show the differences between both samples. As the applied magnetic fields were applied off-plane (increasing angles), H_C increases whereas M_R decreases (Fig. 4 c and d). Py/NC sample exhibits higher H_C and M_R compared to those of Py/PEEK sample. These values confirm the existence of a global in-plane easy axis for both samples.

FIG. 4 HERE

Py/PEEK presents a widening of the in-plane and out-of-plane hysteresis loops in comparison to rigid flat films. The thickness [12], [31], [32] of the deposited Py, and the roughness [29]-[31] of both Py and substrate, cause changes in the anisotropy and H_C and M_R values [29]-[32]. However, these atypical responses can be ascribed to the Py deposited on the detected crinkles on PEEK that will generate a pinning of domain walls and an anomalous magnetization reversal from that expected from a homogeneous Py thin film [32]. Py/NC sample exhibits higher H_C (Fig. 4c), a much more squared hysteresis loop, in terms of higher M_R/M_S values, for in-plane and out-of-plane hysteresis loops compared to Py/PEEK sample. These increased values of H_C and M_R/M_S for all the measured hysteresis loops point out the effect of the nanostructure in the magnetization reversal process. In order to obtain extended information about the magnetization reversal dynamics FORC analysis were performed in-plane orientation for both samples. The resulting FORC diagrams are presented in Fig. 5.

FIG. 5 HERE

FORC technique and details on its analysis can be found elsewhere [33]-[35]. Briefly, based on the classical Preisach model, FORC analysis models the hysteresis as a set of independent mathematical hysterons. Each hysteron is characterized by their coercivity, H_C^F and bias field H_U. Hysterons provide statistical information about the magnetic behavior of the whole system and at the same time, they allow to de-convolute some of the individual magnetic characteristic from the interaction field among the whole sample. Before calculating the density function (ρ) (1), magnetization values (M) were normalized to M_s of each sample, and thus, intensities are relative for the maximum of each sample.

$$\rho(H, H_R) = -\frac{1}{2}\frac{\partial^2 M}{\partial H \partial H_R} \quad (H \geq H_R) \tag{1}$$

The FORC distributions are represented using a new coordinate system that essentially consists of the local coercivities (H_C^F) and the bias or interaction field (H_U). The new coordinated system (2) is 45º rotated from the (H, H_R).

$$H_C^F = \frac{H - H_R}{2} \quad \text{and} \quad H_U = \frac{H + H_R}{2} \tag{2}$$

Taking into account this, H_C^F is then an indicator for the energy required for achieving this specific magnetization change, but not necessarily a true coercive field.

Py/PEEK sample FORC distribution (Fig. 5 a) presents positive values a long H_C^F axis, that extends up to 1.2 kA/m. This distribution exhibit, almost symmetric, low H_U values pointing to a low interactions eg. magnetostatic, within the sample. This distribution is similar to that reported previously for Py thin fims [36]-[37]. However, there is an additional negative distribution that also extend along H_C axis but with increased negative H_U values. The existence of this distribution should be ascribed to the previously mentioned Py on the crinkles. The density distribution of Py/NC in Fig. 5 b) shows noticeable variations compared to that of Py/PEEK. The distribution also extends along H_C^F axis reaching up to 3.4 kA/m. This is indicative of a broader population of hysterons with different coercive fields. This fact can be ascribed to the broad size distribution of nanodomes (see Fig. 4 d). In addition, the distribution that asymmetrically extends >2 kA/m along H_U is also remarkable. In this case, this increment in the interaction fields should be related to the possible generation of magnetostatic interactions between adjacent nanodomes. However, more complex interactions should not be ruled out as there are also negative distributions located at H_C^F 0.3 kA/m and H_U 1 and -1.75 kA/m. These changes in the FORC distributions clearly points out the important modifications that the generated nanodome structure induce in the magnetization process.

After the first magnetic characterization the samples were submitted to 10 mechanical bending cycles. The hysteresis loops maintain similar characteristics for both samples with no evident changes neither in M_R and H_C values or shape.

Finally, and in order to evaluate the resistance of Py to separate from PEEK and NC, the ISO 2409 tests were adapted to be performed in these samples. For this test we did not applied cuts on their surfaces. Note that this test is a pass/fail test and it does not provide absolute values of adhesion. Some images of the results are shown in Fig. 6.

FIG. 6 HERE

Fig. 6 shows the resulting first transparent adhesive tape after the test. Fig. 6 a) corresponds to Py/PEEK sample. Few

scattered particles of Py were detected on the adhesive tape. The appearance of these particles in the first adhesive tape was expected since no cleanroom conditions were applied before and after to Py deposition and thus, some of these particles may adhere during the first stage of tests. The following tests, employing incremental adhesive tapes did not remove any significant amount of material (under the applied magnification) from the sample surface. Thus, Py/PEEK sample passed the tests. This extraordinary adhesion Fig. 6 b) shows the results for the Py/NC sample. In this case, the detached Py layer is evident for continuous and large areas of the sample. Therefore, Py/NC sample failed the test.

IV. Conclusion

A new approach to synthesize bendable nanostructured magnetic surface has been presented. The advantages of this approach are cost and time savings with reductions in hazardous chemical reagents compared to previous techniques. Magnetic properties of Py sputtered thin films on PEEK (Py/PEEK) and on TiO_2 nanotubes layers in PEEK (Py/NC) have been characterized. The increase in H_C and M_R due to the nanostructure formed by nanodomes has been verified. FORC analysis revealed also increased magnetic interactions due to the nanostructure. The adhesion tests revealed an extraordinary adhesion of sputtered Py on PEEK without pretreatment of PEEK. The adhesion of Py on NC surfaces is lower compared to that of bare PEEK. Nevertheless, Py/PEEK and Py/NC samples do not degrade magnetic properties after bending cycles. Therefore, Py/NC represents a valid choice if high level of adhesion is not required.

The obtained results can be considered a promising starting point for future integration of functional magnetic nanostructures in shapeable/bendable polymer structures. In addition, it offers new possibilities in basic research to study magnetic nanostructures in curved surfaces on robust substrates.

Acknowledgment

This work was supported by: the Karlsruhe Nano Micro Facility (KNMF) a Helmholtz Research Infrastructure at Karlsruhe Institute of Technology, the FP7 Project WATER (G.A. 316082), Grants PID2020-117024GB-C42 and PID2020-115325GB-C31 funded by MCIN/AEI/ 10.13039/501100011033 and would like to acknowledge ICTS Micronanofabs.

References

[1] D. Makarov, O. M. Volkov, A. Kákay, O. V. Pylypovskyi, B. Budinská, and O. V. Dobrovolskiy, "New Dimension in Magnetism and Superconductivity: 3D and Curvilinear Nanoarchitectures". *Adv. Mater.*, vol. 34, 2101758, 2022.

[2] E. Berganza, J.A. Fernandez-Roldan, M. Jaafar, A. Asenjo, K. Guslienko and O. Chubykalo-Fesenko "3D quasi-skyrmions in thick cylindrical and dome-shape soft nanodots". *Sci Rep* vol. 12, 3426, 2022.

[3] E. Berganza, M. Jaafar, J. A. Fernandez-Roldan, M. Goiriena-Goikoetxea, J. Pablo-Navarro, A. García-Arribas, K. Guslienko, C. Magén, J. M. De Teresa, O. Chubykalo-Fesenko and A Asenjo. "Half-hedgehog spin textures in sub-100 nm soft magnetic nanodots" *Nanoscale*, vol. 12, 18646, 2020.

[4] R. V. Verba, D. Navas, A. Hierro-Rodriguez, S. A. Bunyaev, B. A. Ivanov, K. Y. Guslienko, G. N. Kakazei, "Overcoming the Limits of Vortex Formation in Magnetic Nanodots by Coupling to Antidot Matrix", *Phys. Rev. Applied*, vol. 10, 3, 031002, 2018.

[5] J. C. Costa, F. Spina, P. Lugoda , L. Garcia-Garcia, D. Roggen and N. Münzenrieder "Flexible Sensors—From Materials to Applications", *Technologies*, vol. 7, 35, 2019

[6] V. T. Rathod, J. S. Kumar and A. Jain "Polymer and ceramic nanocomposites for aerospace applications", *Appl. Nanosci.*, vol. 7, pp. 519–548, 2017.

[7] M. Thiruchitrambalam, D. Bubesh Kumar, D. Shanmugam and M. Jawaid, "A review on PEEK composites – Manufacturing methods, properties and applications" *Materials Today: Proceedings*, vol. 33, Part 1, pp 1085-1092, 2020.

[8] C. Wang, W. Su, J. Pu, Z. Hu and M. Liu, "A Self-biased Anisotropic Magnetoresistive (AMR) Magnetic Field Sensor on Flexible Kapton," *2018 IEEE International Magnetics Conference (INTERMAG)*, 2018, pp. 1-1.

[9] K. Agra, T. J. A. Mori, L.S. Dorneles, V. M. Escobar, U. C. Silva, C. Chesman, F. Bohn, M. A. Corrêa, "Dynamic magnetic behavior in non-magnetostrictive multilayered films grown on glass and flexible substrates", *J. Magn. Magn.*, vol. 355, pp. 136-141, 2014

[10] B. Li, M. N. Kavaldzhiev, J. Kosel, "Flexible magnetoimpedance sensor",*J. Magn. Magn. Mater.*, vol. 378, pp. 499–505, 2015.

[11] A. García-Arribas, L. Combarro, M. Goiriena-Goikoetxea, G. V. Kurlyandskaya, A. V. Svalov, E. Fernández, I. Orue, J. Feuchtwange, "Thin-Film Magnetoimpedance Structures Onto Flexible Substrates as Deformation Sensors," *IEEE Trans. Magn.*, vol. 53, no. 4, pp. 1-5, 2017

[12] C. M. Madrid Aguilar, A. V. Svalov, A. A. Kharlamova, E. E. Shalygina, A. Larrañaga, I. Orue, G. V. Kurlyandskaya, "Magnetic and Microwave Properties of FeNi Thin Films of Different Thicknesses Deposited Onto Cyclo Olefin Copolymer Flexible Substrates," *IEEE Trans. Magn.*, vol. 58, no. 2, pp. 1-5, 2022.

[13] S. M. Kurtz, J. N. Devine, "PEEK biomaterials in trauma, orthopedic, and spinal implants", *Biomaterials*, vol 28, pp 4845-4869, 2007.

[14] M. Ferrara, M. Rinaldi, L. Pigliaru, F. Cecchini,, F. Nanni, *J. Appl. Polym. Sci*., vol. 139, e52150, 2022.

[15] M. Rinaldi, F. Cecchini, L. Pigliaru, T. Ghidini, F. Lumaca, F. Nanni, "Additive Manufacturing of Polyether Ether Ketone (PEEK) for Space Applications: A Nanosat Polymeric Structure". *Polymers* vol. 13, 11, 2021.

[16] J. Martin and M.S. Martín-González "The use of PEEK nanorod arrays for the fabrication of nanoporous surfaces under high temperature: SiNx example". *Nanoscale*, vol. 4, 5608, 2012.

[17] J. Martín, M. Hernández-Vélez, C. Luna, A. Muñoz, M. Vázquez and C Mijangos "Fabrication and characterization of polymer-based magnetic composite nanotubes and nanorods", *Eur. Polym. J.*, vol. 48, pp. 712-719. 2012.

[18] M. Worgull, *Hot Embossing − Theory and Technology of Micro Replication*; William Andrew: Oxford, U.K., 2009.

[19] A. Ruiz-Clavijo, O. Caballero-Calero, M. Martin-Gonzalez, "Revisiting anodic alumina templates: from fabrication to applications", *Nanoscale*, vol. 13, 4, pp. 2227-2265, 2021.

[20] O. Caballero-Calero; M. Martín-González, "3D porous alumina: a controllable platform to tailor magnetic nanowires". *Magnetic Nano-and Microwires*. Woodhead Publishing, 2020. pp. 3-20.

[21] W. O. Rosa, M. Jaafar, A. Asenjo and M Vázquez, "Nanostructured Co film on ordered polymer nanohills: a base for novel magnetic nanostructures", *Nanotechnology* vol. 20, 075301, 2009.

[22] S. Michea, S. Oyarzún, S. Vidal, and J. Denardin, "Enhanced Hall effect in Co/Pd multilayered nanodomes with perpendicular anisotropy". *AIP Advances*. Vol. 7. pp. 56310-56310, 2017.

[23] D. W. Shi, P. K. Greene, P. Liu, K. Javed, K. Liu and X. F. Han, "Co/Pt Multilayers on Self-Organized Hexagonal Patterned Nanodots," in *IEEE Trans. Magn.*, vol. 50, no. 11, pp. 1-4, 2014, Art no. 2303004.

[24] A. Ruiz-Clavijo, S. Ruiz-Gomez, O. Caballero-Calero, L. Perez, and M. Martin-Gonzalez, M., "Tailoring Magnetic Anisotropy at Will in 3D Interconnected Nanowire Networks", *Phys. Status Solidi RRL*, vol. 13: 1900263, 2019.

[25] A. Ruiz-Clavijo, O. Caballero-Calero, D. Navas, A. A. Ordoñez-Cencerrado, J. Blanco-Portals, F. Peiró, R. Sanz, M. Martín-González "Unveiling the complex magnetization reversal process in 3D Nickel Nanowire Networks", *Adv. Electron. Mater.* 2200342, 2022.

[26] P. Roy, S. Berger, and P. Schmuki. "TiO_2 Nanotubes: Synthesis and Applications" *Angew. Chem. Int. Ed.*, vol. 50, pp 2904 – 2939, 2011.

[27] R. Sanz, M. A. Buccheri, M. Zimbone, V. Scuderi, G. Amiard, G. Impellizzeri, L. Romano and V. Privitera, "Photoactive layered nanocomposites obtained by direct transferring of anodic TiO_2 nanotubes to commodity thermoplastics", *Appl. Surf. Sci.*, vol. 399, pp. 451-462, 2017.

[28] *ISO 2409:2020 Paints and varnishes Cross-cut test*. International Organization for Standardization. CH-1214 Vernier, Geneva.

[29] M. Belusky, S. Lepadatu, J. Naylor and M.M. Vopson, "Evidence of substrate roughness surface induced magnetic anisotropy in $Ni_{80}Fe_{20}$ flexible thin films", *J. Magn. Magn. Mater.*, vol. 478, pp. 77-83, 2019.

[30] J. Rittinger, P. Taptimthong, L. Jogschies, M. C. Wurz, and L. Rissing "Impact of different polyimide-based substrates on the soft magnetic properties of NiFe thin films", *Proc. SPIE 9517, Smart Sensors, Actuators, and MEMS VII; and Cyber Physical Systems*, 95171R (21 May 2015);

[31] M. M. Vopson, J. Naylor, T. Saengow, E.G. Rogers, S. Lepadatu, and Y.K. Fetisov, "Development of flexible $Ni_{80}Fe_{20}$ magnetic nano-thin films", *Physica B Condens. Matter.*, vol. 525, pp. 12-15, 2017.

[32] M. Romera, R. Ranchal, D. Ciudad, M. Maicas, and C. Aroca "Magnetic properties of sputtered Permalloy/molybdenum multilayers" *J. Appl. Phys.* 110, 083910, 2011.

[33] I. Mayergoyz, "Mathematical models of hysteresis," in *IEEE Trans. Magn.*, vol. 22, no. 5, pp. 603-608, 1986.

[34] A. P. Roberts, D. Heslop, X. Zhao and C. R. Pike, "Understanding fine magnetic particle systems through use of first-order reversal curve (FORC) diagrams" *Rev. of Geophys.*, vol. 52, 4, 2014.

[35] C. I. Dobrota, and A. Stancu, "What does a first-order reversal curve diagram really mean? A study case: Array of ferromagnetic nanowires" *J. Appl. Phys.* vol. 113, 043928, 2013.

[36] J. Gräfe, M. Schmidt, P. Audehm, G. Schütz, and E. Goering "Application of magneto-optical Kerr effect to first-order reversal curve measurements" *Rev. Sci. Instrum.* vol. 85, 023901, 2014.

[37] L. Alonso, T.R.F. Peixoto and D. R. Cornejo "Magnetic interaction in exchange-biased bilayers: a first-order reversal curve analysis" J. *Phys. D: Appl. Phys.* vol. 43, 465001, 2010.

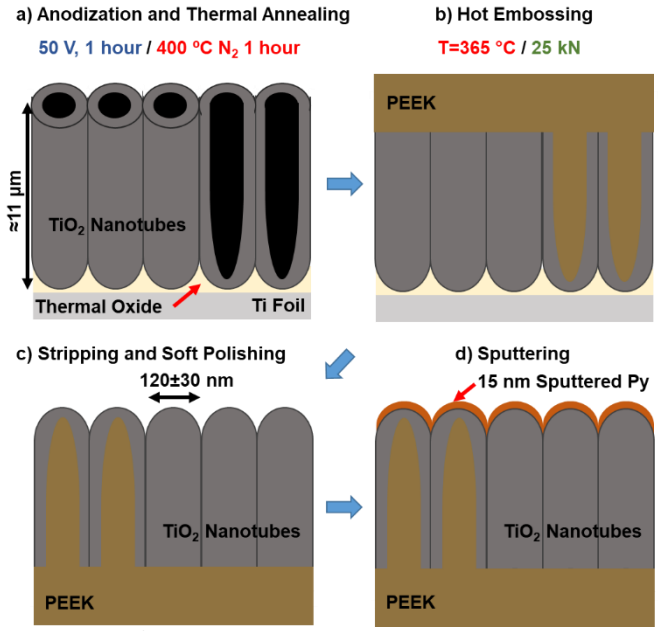


Fig. 1. Sketch of the employed synthesis processes.

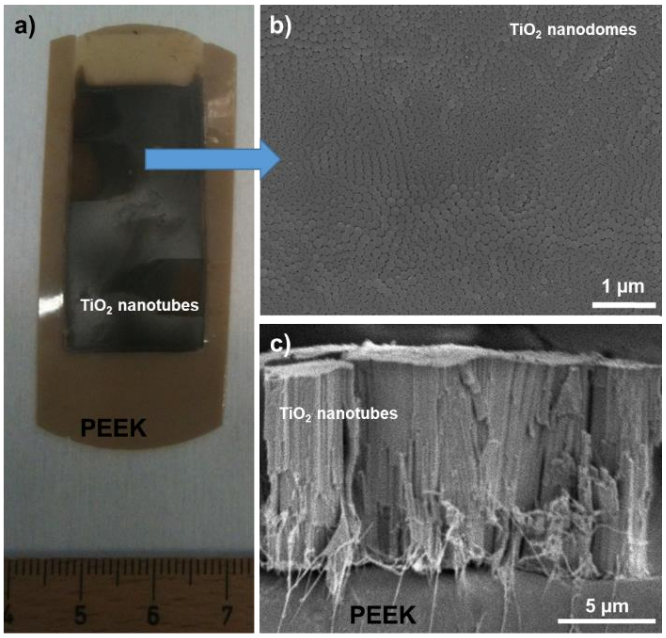


Fig. 2. a) Image of resulting NC after stripping process. Scale in cm. b) SEM image of the NC surface after the stripping process and soft polishing steps. c) Cross section image of the NC after soft polishing step.

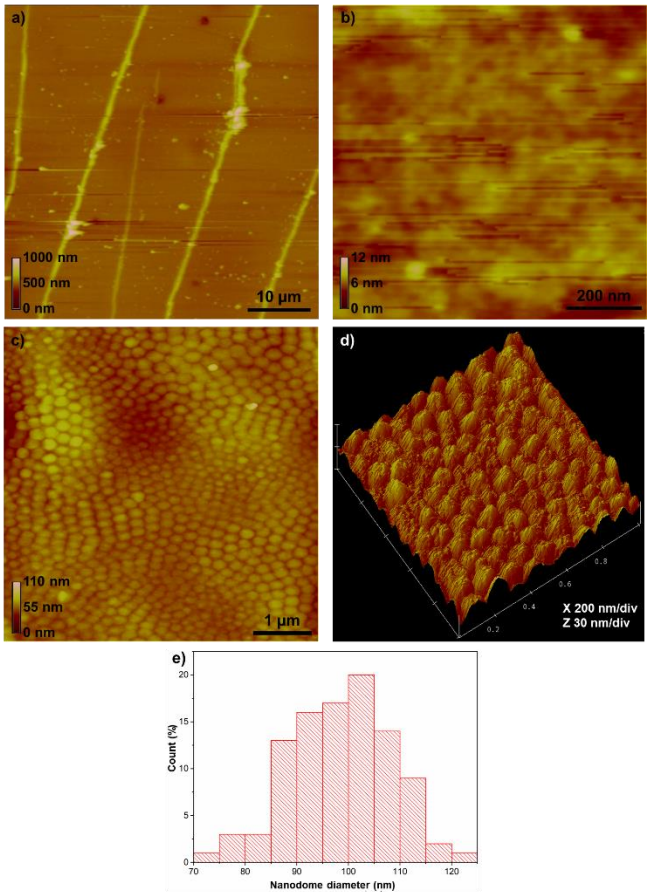


Fig. 3. AFM images of Py/PEEK samples a) and b). Py/NC c) and d). e) Resulted statistical diameter distribution of nanodomes from image c).

IEEE Copyright C. Martín-Rubio et al., "Magnetic Characterization of Permalloy Nanodome Surfaces on Flexible PEEK/TiO2 Vertical Nanotubes Composites," in IEEE Transactions on Magnetics, vol. 59, no. 2, pp. 1-6, Feb. 2023, Art no. 6500106, https://doi.org/10.1109/TMAG.2022.3212831

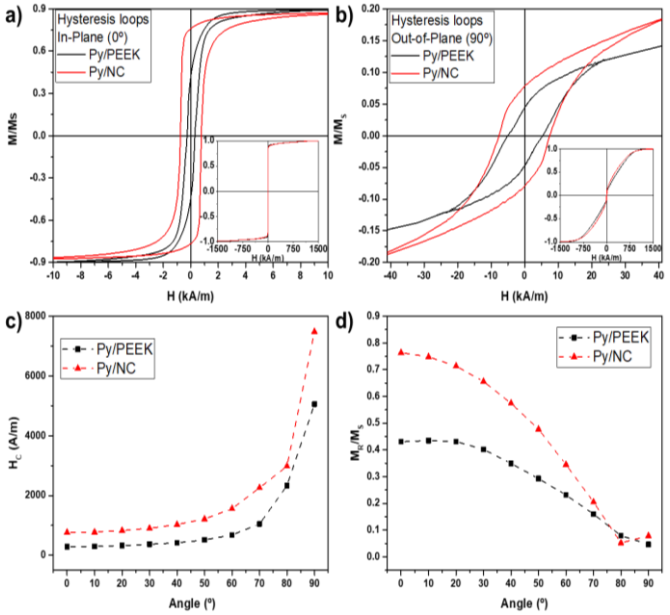


Fig. 6. Detailed hysteresis loops of Py/PEEK and Py/NC samples at a) In-Plane (0°) and b) Out-of-plane (90°). Insets in a) and b) shows the complete hysteresis loops. Obtained H_C c) and M_R/M_S d) values of the measured hysteresis loops at different angles of applied field. The dash-dotted lines in c) and d) are guide for the eye.

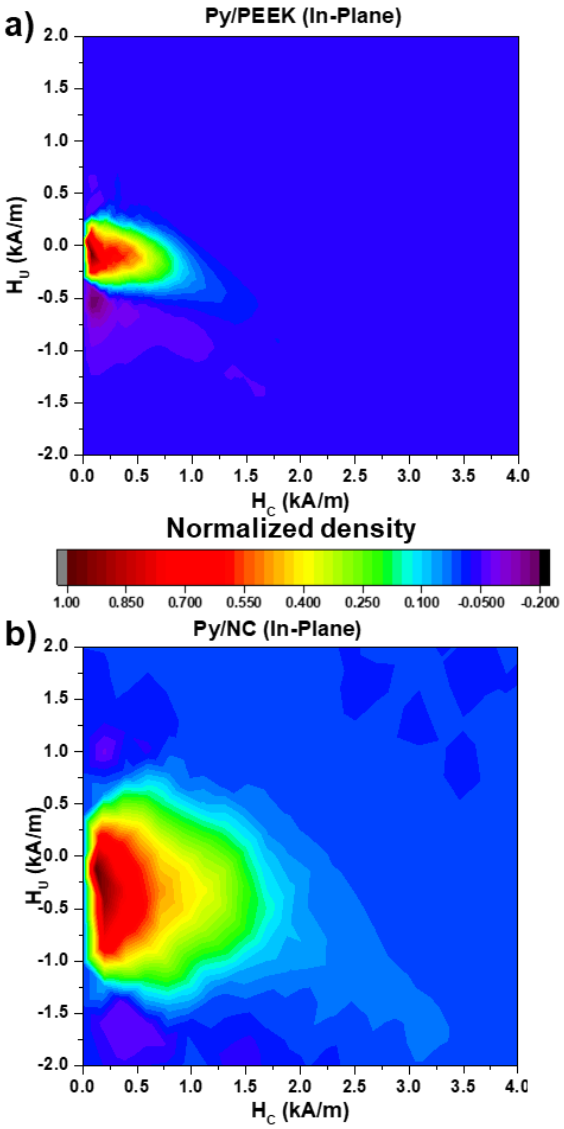


Fig. 5. FORC diagrams measured in In-plane orientation a) Py/PEEK sample and b) Py/NC sample. The density scale bar is common for both configurations.

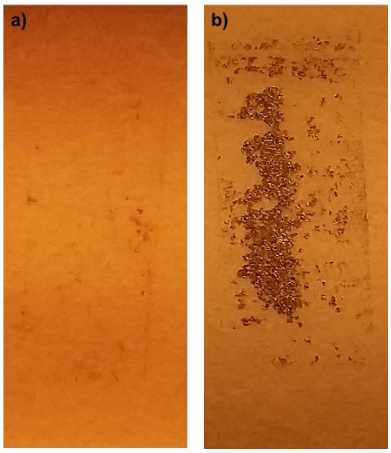


Fig. 6. ISO 2409 results on the 1x2 cm samples. Images of adhesive tape after the test a) Py/PEEK sample and b) Py/NC sample.